Published OnlineFirst September 9, 2016; DOI: 10.1158/0008-5472.CAN-16-2141

Microenvironment and Immunology

Cancer Research

Agonistic CD40 mAb-Driven IL12 Reverses Resistance to Anti-PD1 in a T-cell–Rich Tumor

Shin Foong Ngiow[1,2], Arabella Young[1,2], Stephen J. Blake[3], Geoffrey R. Hill[4,5], Hideo Yagita[6], Michele W. L. Teng[2,3], Alan J. Korman[7], and Mark J. Smyth[1,2]

Abstract

The durability and efficacy of anti-human PD1 monoclonal antibodies (PD1 mAb) vary across different malignancies. Although an absence of tumor-infiltrating cytotoxic T lymphocytes has been identified as a cause for resistance to PD1 mAb, the presence of intratumor exhausted PD1^{hi} T cells also contributes to insensitivity to this immune checkpoint therapy. In this study, we used mouse tumor models of PD1 mAb resistance that harbored PD1^{hi} T cells and flow cytometry analysis of tumor-infiltrating leukocytes immediately post-therapy as a screening platform to identify agents that could resensitize T cells to PD1 blockade. We showed that an agonistic anti-CD40 mAb converted PD1^{hi} T cells into PD1^{lo} T cells, reversing phenotypic T-cell exhaustion and allowing the anti-PD1 refractory tumors to respond to anti-PD1 therapy. PD1 downmodulation by anti-CD40 mAb relied upon IL12 but not IL23, CD80/CD86/CD28, or CD70/CD27. Consistent with a role for regulatory T cells (Treg) in promoting T-cell exhaustion, we also showed that intratumor Treg presented with a less activated and attenuated suppressive phenotype, marked by reductions in CTLA4 and PD1. Similar to anti-CD40 mAb, anti-CTLA4 mAb also lowered intratumor T-cell PD1 expression. Our study provides a proof-of-principle framework to systematically identify immune conditioning agents able to convert PD1^{hi} T cells to PD1^{lo} T cells, with clinical implications in the management of anti-PD1 refractory patients. *Cancer Res; 76(21); 6266–77. ©2016 AACR.*

Introduction

Immune checkpoint inhibitors targeting cytotoxic T lymphocyte-associated protein 4 (CTLA4) and program death 1 (PD1) have revolutionized the oncology field. Despite the clinical successes of anti-human PD1 mAbs (pembrolizumab or nivolumab) in treating patients with melanoma, non–small cell lung cancer (NSCLC), renal cell carcinoma, and other malignancies, the durability and efficacy of this therapy varies (1–6). Preclinical and clinical studies showed a positive correlation between high levels of mutational burden or presence of neoantigens in cancer and anti-PD1 therapeutic responsiveness (7–10). In NSCLC patients, CD8$^+$ T cells reactive to these clonal neoantigens were detected infiltrating tumors, and their presence was associated with enhanced sensitivity to anti-PD1 mAb (9). A similar correlation was also reported in melanoma patients treated with pembrolizumab (5). Given that PD1 expression is mainly found on intratumor T cells, it is anticipated that the lack of tumor-infiltrating CD8$^+$ T cells is one of the major reasons for anti-PD1 insensitivity (11). In this light, a huge effort is currently being undertaken in the field to utilize different therapeutic approaches to increase intratumor CD8$^+$ T cells to improve the durability and efficacy of anti-PD1/PDL1 therapy (12–14).

We recently demonstrated that PD1^{hi} CD8$^+$ T cells act as a biomarker of resistance to anti-PD1 therapy in mouse tumor models (15), with a similar T-cell phenotype observed in tumor-infiltrating leukocytes from NSCLC patients (16). In contrast, anti-PD1 mAb showed good antitumor efficacy in tumor models infiltrated by PD1^{lo} CD8$^+$ T cells (15). It is worth noting that this biology of anti-PD1 resistance and sensitivity also exists in the context of viral immunity, where terminally exhausted CD8$^+$ PD1^{hi} T cells were also shown to be insensitive to PD1/PDL1 blockade (17). These studies highlighted the relevance of this PD1 regulation machinery in T cell–mediated inflammatory diseases. Interestingly, we also showed that intratumor CD8$^+$ PD1^{hi} T-cell exhaustion was reversible when Foxp3$^+$ regulatory T cells (Treg) were conditionally depleted, with these PD1^{hi} T cells rapidly transitioning to a PD1^{lo} phenotype (15). This Treg depletion-driven reversal of exhaustion was also reported in a mouse model of chronic lymphocytic choriomeningitis virus (LCMV) infection, although the transition from PD1^{hi} to PD1^{lo} was not assessed (18). While complete Treg depletion can be performed using genetically modified mouse models (15, 18), its feasibility

[1]Immunology in Cancer and Infection Laboratory, QIMR Berghofer Medical Research Institute, Herston, Queensland, Australia. [2]School of Medicine, University of Queensland, Herston, Queensland, Australia. [3]Cancer Immunoregulation and Immunotherapy Laboratory, QIMR Berghofer Medical Research Institute, Herston, Queensland, Australia. [4]Bone Marrow Transplant Laboratory, QIMR Berghofer Medical Research Institute, Brisbane, Queensland, Australia. [5]Department of Haematology and Bone Marrow Transplantation, Royal Brisbane and Women's Hospital, Butterfield St, Brisbane, Queensland, Australia. [6]Department of Immunology, Juntendo University School of Medicine, Tokyo, Japan. [7]Bristol Myers Squibb Company, Redwood City, California.

Note: Supplementary data for this article are available at Cancer Research Online (http://cancerres.aacrjournals.org/).

S.F. Ngiow and A. Young contributed equally to this article.

Current address for S.F. Ngiow: Department of Microbiology and Institute for Immunology, University of Pennsylvania Perelman School of Medicine, Philadelphia, PA.

Corresponding Authors: Mark J. Smyth, QIMR Berghofer Medical Research Institute, 300 Herston Road, Herston, 4006, Australia. Phone: 61-7-3845-3957; Fax: 61-7-3362-0111; E-mail: mark.smyth@qimrberghofer.edu.au; and Shin Foong Ngiow, shinfoong.ngiow@qimrberghofer.edu.au

doi: 10.1158/0008-5472.CAN-16-2141

in the clinic remains limited. In this light, we explored alternate therapeutic strategies that could modulate T-cell PD1 expression levels and/or reverse its exhaustion state.

Here, using the established AT3 tumor harboring PD1^{hi} intratumor T cells, we identify that an agonistic anti-CD40 mAb rapidly lowered T-cell PD1 expression. This reversal of T-cell exhaustion was marked by increases in T-cell cytokine-producing, cytotoxic, and proliferative capacities, together with a reactivated T-cell phenotype. We identify that anti-CD40–driven IL12 cytokine production regulates T-cell PD1 expression, independent of enhanced costimulatory signaling on T cells. Strikingly, this immune-conditioning therapy rendered this resistant tumor sensitive to anti-PD1 therapy.

Materials and Methods

Mice

C57BL/6 and Balb/c wild-type (WT) were purchased from the ARC Animal Resources Centre. C57BL/6 IL23p19-deficient mice (19) were bred in-house at the QIMR Berghofer Medical Research Institute and used between the ages of 6 and 16 weeks. Groups of 3 to 8 mice per experiment were used for experimental assays, to ensure adequate power to detect biological differences. All experiments were approved by the QIMR Berghofer Medical Research Institute Animal Ethics Committee.

Tumor cell lines

The C57BL/6 AT3 mammary adenocarcinoma (obtained from Dr. Trina Stewart in 2009, Peter MacCallum Cancer Centre, Melbourne, Australia) and BALB/c Renca renal carcinoma (obtained from Dr. Thomas Sayers in 1991, Frederick Cancer Research Facility, Frederick, MD) were maintained as previously described (15). The AT3 and Renca cell lines were tested negative for mycoplasma, but not tested for genetic authenticity in the past 5 years. For *in vivo* experiments, 1×10^6 (AT3) or 2×10^5 (Renca) tumor cells were subcutaneously injected into mice in a 100 μL volume.

Antibodies and reagents

Purified anti-mouse CD40 mAb (FGK4.5; 100 μg, unless indicated otherwise), PD1 mAb (RMP1-14; 250 μg), CD73 (TY/23; 250 μg), CD137 (3H3; 100 μg), DR5 (MD5-1; 100 μg), GITR (DTA-1; 250 μg), OX40 (OX86; 250 μg), and control Ig (2A3; 250 μg; cIg) were purchased from BioXCell (West Lebanon). Anti-IL12p40 mAb (C17.8; 500 μg), PDL2 (TY25; 250 μg), and IL10R (1B1.3; 500 μg) were produced in-house. Anti-CTLA4 (9D9-IgG2a; 200 μg) was kindly provided by Dr. Alan Korman (BMS). Anti-CD27 (RM27-3E5; 100 μg) was kindly provided by Dr. Hideo Yagita (Jutendo University, Bunkyo, Tokyo, Japan). Anti-CD28 (37.51; 100 μg) was kindly provided by Dr. Geoff Hill (QIMR Berghofer Medical Research Institute, Brisbane, Australia). A2A adenosine receptor inhibitor (A2ARi; SCH58261; 10 mg/kg for 3 consecutive days) was purchased from Sigma. Recombinant IL12 (1 μg) and IL18 (1 μg) were purchased from eBioscience and R&D Systems, respectively. All antibodies and reagents were used at the dose as indicated (intraperitoneally), and tumor tissues were harvested 48 to 72 hours (unless otherwise indicated) after therapy for flow cytometry analysis.

In vivo treatments

AT3 and Renca tumor growth was measured using a digital caliper, and tumor sizes are presented as mean ± SEM. For flow cytometry analyses of intratumor immune cells, mice bearing established AT3 tumor (days 14–19; 25–45 mm^2) or Renca (Days 7–10; 10–25 mm^2) were treated with the indicated antibodies or reagents and immune cells were isolated 48 to 72 hours post treatment.

Flow cytometry analysis

Tumors tissues were harvested from mice that had been treated with mAb or otherwise and processed for flow cytometry analysis as previously described (20). For surface staining, tumor-filtrating leukocytes (TIL) were stained with eFluor780 anti-CD45.2 (104; eBioscience), eFluor450 or Brilliant Violet 605 anti-CD4 (RM4-5; eBioscience and Biolegend), PE-Cy7 or Brilliant Violet 421 anti-CD8a (53-6.7; eBioscience and Biolegend), FITC or PE anti-TCRβ (H57-597; eBioscience), PE-Cy7-anti-CD11b (M1/70; eBioscience), eFluor450-anti-Gr1 (RB6-8C5; eBioscience), FITC- or PE-anti-PD1 (J43; eBioscience and BD Pharmingen), APC-anti-PDL1 (10F.9G2; Biolegend), PE-anti-CD27 (LG.3A10; BD Pharmingen), PE-anti-CD86 (GL1; BD Pharmingen), APC-anti-CD80 (16-10A1; eBioscience), PE-anti-CD70 (FR70; BD Pharmingen), FITC-anti-CD40 (HM40-3; BD Pharmingen), Biotin-conjugated-anti-CD28 (37.51; Biolegend), PE-Cy7- or APC-conjugated streptavidin (eBioscience), Alexa Fluor 488-anti-CD25 (PC61.5; eBioscience), Brilliant Violet 605-anti-CD127 (A7R34; Biolegend), PE-Cy7-anti-CD278 (ICOS; 7E.17G9; eBioscience), APC-anti-CD223 (Lag3; C9B7W; Biolegend), PE-anti-CD366 (Tim3; RMT3-23; Biolegend), APC-anti-TIGIT (1G9; Biolegend), PE-Cy7 anti-CD39 (24DMS1; eBioscience), PE-anti-CD73 (TY/23; BD Pharmingen), APC-anti-CD44 (IM7; Biolegend), FITC-anti-CD62L (MEL-14; Biolegend), and respective isotype antibodies in the presence of anti-CD16/32 (2.4G2). 7AAD (Biolegend) or Zombie Aqua Fixable Viability Kit (Biolegend) was used to exclude dead cells. For intracellular transcription factor staining, surface-stained cells were fixed and permeabilized using the Foxp3/Transcription Factor Staining Buffer Set (eBioscience), according to the manufacturer's protocol, and stained using eFluor450-anti-Foxp3 (FJK-16s, eBioscience), FITC-anti-Tbet (4B10; Biolegend), APC-anti-CTLA4 (UC10-4B9, eBioscience), Alexa Fluor 647-anti-Ki67 (B56), eFluor660-anti-Eomes (Dan11mag; eBioscience), and respective isotype antibodies. For intracellular staining of IFNγ/TNF or IL12p40, cells were stimulated *in vitro* with 50 ng/mL PMA (Sigma Aldrich) and 1 μg/mL ionomycin (Sigma Aldrich), or 100 ng/mL LPS, respectively in the presence of GolgiPlug (BD Biosciences) for 4 hours, and then surface stained as aforementioned. Surface-stained cells were then fixed and permeabilized using BD Cytofix/Cytoperm (BD Biosciences) according to the manufacturer's protocol, and stained with PE-anti-IL12p40 (C15.6; BD Pharmingen), PE-anti-IFNγ (XMG1.2; eBioscience), Alexa Fluor 647-anti-granzyme B (GB11; BD Pharmingen), and Brilliant Violet 605-anti-TNF (MP6-XT22; Biolegend), and respective isotype antibodies. Cells were acquired on the BD FACSCANTO II and LSR (BD Biosciences) and analysis was carried out using FlowJo (Tree Star).

Statistical analyses

Statistical analyses were carried out using Graph Pad Prism software. Significant differences in tumor growth were determined by an unpaired *t* test. Significant differences in cell subsets were determined by an unpaired *t* test. Values of $P < 0.05$ were considered statistically significant.

Published OnlineFirst September 9, 2016; DOI: 10.1158/0008-5472.CAN-16-2141

Results

Agonistic CD40 mAb regulates T-cell PD1 expression

Recently, we and others have shown that systemic Treg depletion rescued exhausted $CD8^+$ T cells, directly increasing the efficacy of therapeutic T-cell checkpoint blockade in virus and cancer settings (15, 18, 21). Consistent with these findings, we found that an anti-CTLA4 mAb with intratumor Treg-depleting activity (Supplementary Fig. S1A; ref. 22) downregulated PD1 expression on T cells (Supplementary Fig. S1D). Conditioning the AT3 intratumor T cells with anti-CTLA4 from an anti-PD1 resistant $PD1^{hi}$ phenotype to a sensitive $PD1^{lo}$ phenotype results in improved tumor control (Supplementary Fig. S1B; ref. 15). These changes to T-cell PD1 expression also resulted in a further increase in intratumor CD8/Treg ratio in anti-CTLA4+anti-PD1–treated mice (Supplementary Fig. S1C), likely contributing to its superior combinatorial antitumor effect. Coinciding with the reduced PD1 expression on T cells, PDL1 expression was increased on intratumor T cells and myeloid cells (Supplementary Fig. S1E). Supported by this finding, we set out to identify other immune-based target(s) that could rapidly sensitize $PD1^{hi}$ T cell–bearing tumor to anti-PD1 therapy. Given that anti-PD1 mAb alone lowers T-cell PD1 expression (15), only immune targets that achieved $CD8^+$ T-cell PD1 expression below the anti-PD1 mAb–treated threshold were used for further analysis (Fig. 1A and B). From our flow cytometry analyses on TILs isolated 48 to 72 hours post therapy (Fig. 1A and B), an agonistic CD40 mAb was shown to effectively lower intratumor T-cell PD1 expression, in a dose-dependent manner (Fig. 1A and C; Supplementary Fig. S2). In contrast, PDL1 expression was increased on intratumor T cells and myeloid cells (Fig. 1D), in agreement with our previous observation of an inverse correlation of PD1-PDL1 in the tumor microenvironment (15). To confirm the immune conditioning effect of anti-CD40 mAb on anti-PD1 therapy, we treated AT3-bearing mice with a single dose of anti-CD40 mAb prior to the administration of anti-PD1 therapy. In agreement with our previous findings (15), AT3-bearing mice exhibited an anti-PD1 resistant phenotype (Fig. 1E). Similarly, single treatment of anti-CD40 mAb alone did not result in any significant antitumor effect, despite its immune activating function shown in our analyses (Fig. 1E). Strikingly, AT3 tumors were significantly suppressed in mice treated with a single dose of anti-CD40 mAb prior to the commencement of anti-PD1 therapy (Fig. 1E). To assess whether the synergistic effect of anti-CD40 and anti-PD1 mAbs was also present in another tumor model of anti-PD1 resistance, harboring $CD8^+$ $PD1^{hi}$ T cells, we performed similar flow cytometry analyses on TILs isolated from Renca-bearing mice. Interestingly, we found that the proportion of T cells was reduced in anti-CD40 mAb–treated mice (Supplementary Fig. S3A). In contrast to the AT3 tumor model, PD1 expression on T cells isolated from anti-CD40–treated Renca-bearing mice was significantly increased (Supplementary Fig. S3B and S3C). Consistent with the reduction of tumor-infiltrating T cells and induction of higher PD1 expression, we did not measure any synergistic effect of anti-CD40 and anti-PD1 mAbs in Renca-bearing mice (Supplementary Fig. S3D). Nonetheless, just one dose of anti-CD40 alone provided significantly improved tumor control within this model (Supplementary Fig. S3D).

Intratumor T-cell phenotypic changes upon agonistic CD40 mAb therapy

Exhausted $CD8^+$ $PD1^{hi}$ T cells are characterized by the progressive loss of effector functions and expression of different transcription factor profiles in comparison with effector T cells (23, 24). We next asked if T-cell exhaustion in the AT3 tumor is reversed post anti-CD40 therapy. In concordance to the lowered T-cell PD1 expression in anti-CD40–treated AT3-bearing mice, we observed increased proportions of granzyme B-, Ki67-, and IFNγ-expressing T cells, whereas frequency of TNF-expressing T cells was similar between cIg- and anti-CD40–treated mice (Fig. 2A). Consistent with the classical Tbet:Eomes transcriptional profile of $PD1^{hi}$ ($Tbet^{lo}$ $Eomes^{hi}$) and $PD1^{lo}$ ($Tbet^{hi}$ $Eomes^{lo}$) $CD8^+$ T cells (25), we found increased Tbet, but decreased Eomes, in intratumor $CD8^+$ T cells isolated from anti-CD40–treated mice (Fig. 2A). Tbet induction upon anti-CD40 mAb was also observed in intratumor $CD4^+$ T cells, but their Eomes levels were comparable with cIg-treated mice (Fig. 2A). Despite the increased effector functions, $CD4^+$ effector memory T cells ($CD44^+$ $CD62L^-$) were mildly reduced in mice treated with anti-CD40 mAb, whereas the proportions of $CD8^+$ effector memory ($CD44^+$ $CD62L^-$) and central memory ($CD44^+$ $CD62L^+$) T cells were largely unchanged (Fig. 2B). When examining the activation status of intratumor T cells, we detected an increase of CD25- and ICOS-expressing T cells in anti-CD40–treated mice (Fig. 2C and Supplementary S4A). In addition, their intratumor $CD4^+$ T cells also displayed an upregulation of surface IL7 receptor, CD127 (Fig. 2C and Supplementary S4A). Taking all these T-cell parameters into consideration, our data showed that anti-CD40 mAb rapidly induced transcriptional changes to intratumor T cells, and this was accompanied by an increase in their proliferative, cytotoxic, and cytokine-producing capacities.

Altered immune checkpoint receptor expression post anti-CD40 mAb

Another fundamental feature of exhausted T cells is their expression of multiple checkpoint receptors (24, 26). We next sought to determine whether the expression of other T-cell–inhibitory receptors and exhaustion-associated markers was also attenuated by anti-CD40 mAb. We found that anti-CD40 mAb induced higher proportions of Tim3-, TIGIT-, and CD39-expressing $CD4^+$ T cells, and a similar induction was also observed for their Lag3 expression (Fig. 3A and B). In contrast, no significant changes were observed for $CD4^+$ T-cell CD73 expression between cIg- and anti-CD40–treated mice (Fig. 3A and B). Of note, these $TIGIT^+$ $CD4^+$ T cells have lower TIGIT expression as measured by mean fluorescence intensity (MFI; Supplementary S4B). In contrast, $CD39^+$ $CD4^+$ T cells displayed higher CD39 expression post anti-CD40 mAb therapy (Supplementary Fig. S4C). Similar to $CD4^+$ T cells, anti-CD40 mAb also increased Lag3, CD39, and CD73 expression on $CD8^+$ T cells (Fig. 3A and B). However, no significant changes were observed for $Tim3^+$ or $TIGIT^+$ $CD8^+$ T cells between cIg- and anti-CD40–treated mice (Fig. 3A and B). Collectively, these data suggested that anti-CD40 mAb initiates differential regulatory effects for multiple immune receptors on exhausted intratumor T cells.

Anti-CD40 mAb regulates T-cell PD1 status independently of costimulatory ligation

CD40 ligation of antigen presenting cells (APC) stimulates costimulatory ligand expression, providing secondary signals

Published OnlineFirst September 9, 2016; DOI: 10.1158/0008-5472.CAN-16-2141

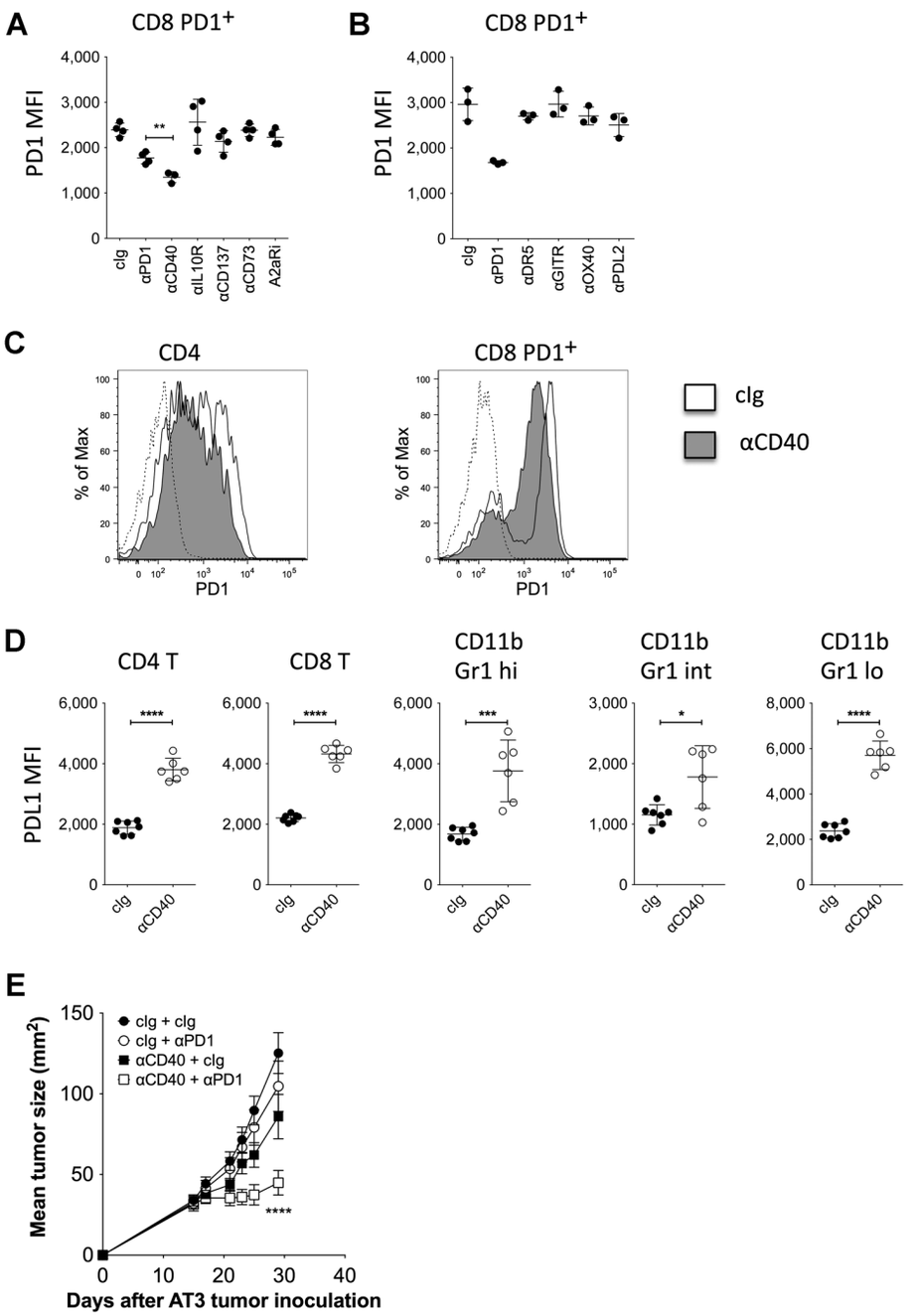

Figure 1.

Anti-CD40 reduces AT3 intratumor T-cell PD1 expression. Groups of B6 WT mice ($n = 3$–5) with established AT3 tumor were treated with the indicated antibody or inhibitor, and tumors were harvested 2 or 3 days after antibody treatments for flow cytometric analyses. **A** and **B,** PD1 MFI of CD8 PD1$^+$ T cells are shown. Statistical differences in CD8$^+$ PD1$^+$ T-cell PD1 MFI between anti-PD1 and anti-CD40–treated mice were determined by an unpaired *t* test (**, $P < 0.01$). **C,** representative overlaid PD1 histogram plots of CD4 (left) and CD8 (right) T cells (dashed histogram, isotype; open histogram, 100 μg of cIg-treated; shaded histogram, 100 μg of anti-CD40–treated) from antibody-treated mice are shown. **D,** PDL1 MFI of indicated TIL subsets between cIg and anti-CD40–treated mice pooled from two independent experiments are shown. Data are presented as mean ± SD. Statistical differences in PDL1 MFI between cIg and anti-CD40–treated mice were determined by an unpaired *t* test (*, $P < 0.05$; ***, $P < 0.001$; ****, $P < 0.0001$). **E,** groups of B6 WT mice ($n = 8$) with established AT3 tumor were treated with 100 μg of cIg or anti-CD40 mAb two days before the commencement of 250 μg of cIg or anti-PD1 mAb. 250 μg of cIg or anti-PD1 was administered every 4 days for a total of 4 doses. Tumor growth was measured using a digital caliper, and tumor sizes are presented as mean ± SEM. Statistical differences in tumor sizes at the indicated time point between control Ig- and anti-CD40 + anti-PD1–treated mice were determined by an unpaired *t* test (****, $P < 0.0001$).

for the generation of a productive T-cell response (27). Given the modulatory effect of anti-CD40 mAb on T-cell PD1 expression in the AT3 tumor model, we next examined whether costimulatory ligation could directly lower T-cell PD1 levels. Our flow cytometry analyses on TILs showed that CD40 was expressed on intratumor CD11b$^+$ Gr1 myeloid cells, particularly on CD11b$^+$ Gr1^{int} and Gr1^{lo} myeloid cells (Fig. 4A). Consistent with reported studies (28, 29), intratumor CD11b$^+$ myeloid cells isolated from anti-CD40-treated mice displayed an increase in CD70, CD80, and/or CD86 expression (Fig. 4A). In concert, we detected downregulation of costimulatory ligand receptors, CD27 and CD28, on intratumor T cells (Fig. 4B). The data indicated a modulated interaction between APC and T cells that may contribute to the regulation of T-cell PD1 status. We then treated AT3-bearing mice with an agonistic anti-CD27 or anti-CD28 mAb, to assess whether the ligation of these receptors could lower T-cell PD1 expression. Notably, however, the administration of anti-CD27 or anti-CD28 mAb did not downregulate PD1 expression on intratumor T cells (Fig. 4C and D). Our findings suggested that the CD80/CD86/CD28 and CD70/CD27 pathways were not involved in mediating the anti-CD40 PD1 downmodulating effect.

Published OnlineFirst September 9, 2016; DOI: 10.1158/0008-5472.CAN-16-2141

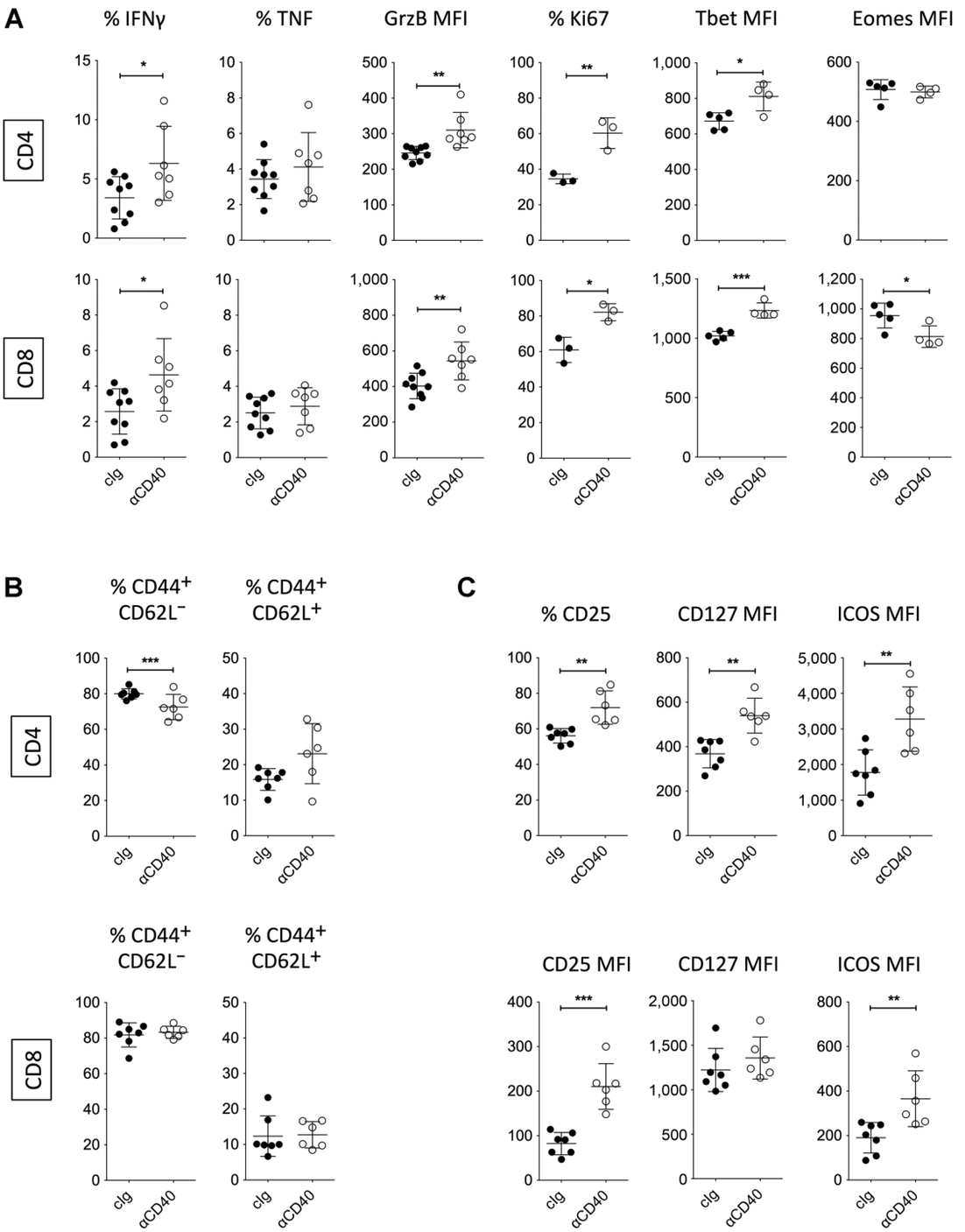

Figure 2.

Anti-CD40 reverses exhaustion of intratumor T cells. Groups of B6 WT mice ($n = 3$–7) with established AT3 tumor were treated with cIg or anti-CD40 mAb, and tumors were harvested 2 or 3 days after antibody treatments for flow cytometric analyses. **A,** frequencies of IFNγ$^+$, TNF$^+$, and Ki67$^+$; and MFIs of granzyme B (GrzB), Tbet, and Eomes in CD4$^+$ (top) and CD8$^+$ (bottom) TILs between cIg- and anti-CD40–treated mice are shown. Data are presented as mean ± SD. Data shown for IFNγ, TNF, and granzyme B are pooled from two independent experiments. Data shown for Tbet and Eomes are representative of two or more independent experiments. **B,** frequencies of CD44$^+$CD62L$^+$ and CD44$^+$CD62L$^-$ in CD4$^+$ (top) and CD8$^+$ (bottom) TILs between cIg- and anti-CD40–treated mice are shown. Data are presented as mean ± SD. **C,** frequencies of CD25$^+$ and MFIs of CD25, CD127, and ICOS in CD4$^+$ (top) and CD8$^+$ (bottom) TILs between cIg- and anti-CD40–treated mice are shown. Data are presented as mean ± SD. Statistical differences in frequencies or MFIs between cIg- and anti-CD40–treated mice were determined by an unpaired *t* test (*, $P < 0.05$; **, $P < 0.01$; ***, $P < 0.001$).

Published OnlineFirst September 9, 2016; DOI: 10.1158/0008-5472.CAN-16-2141

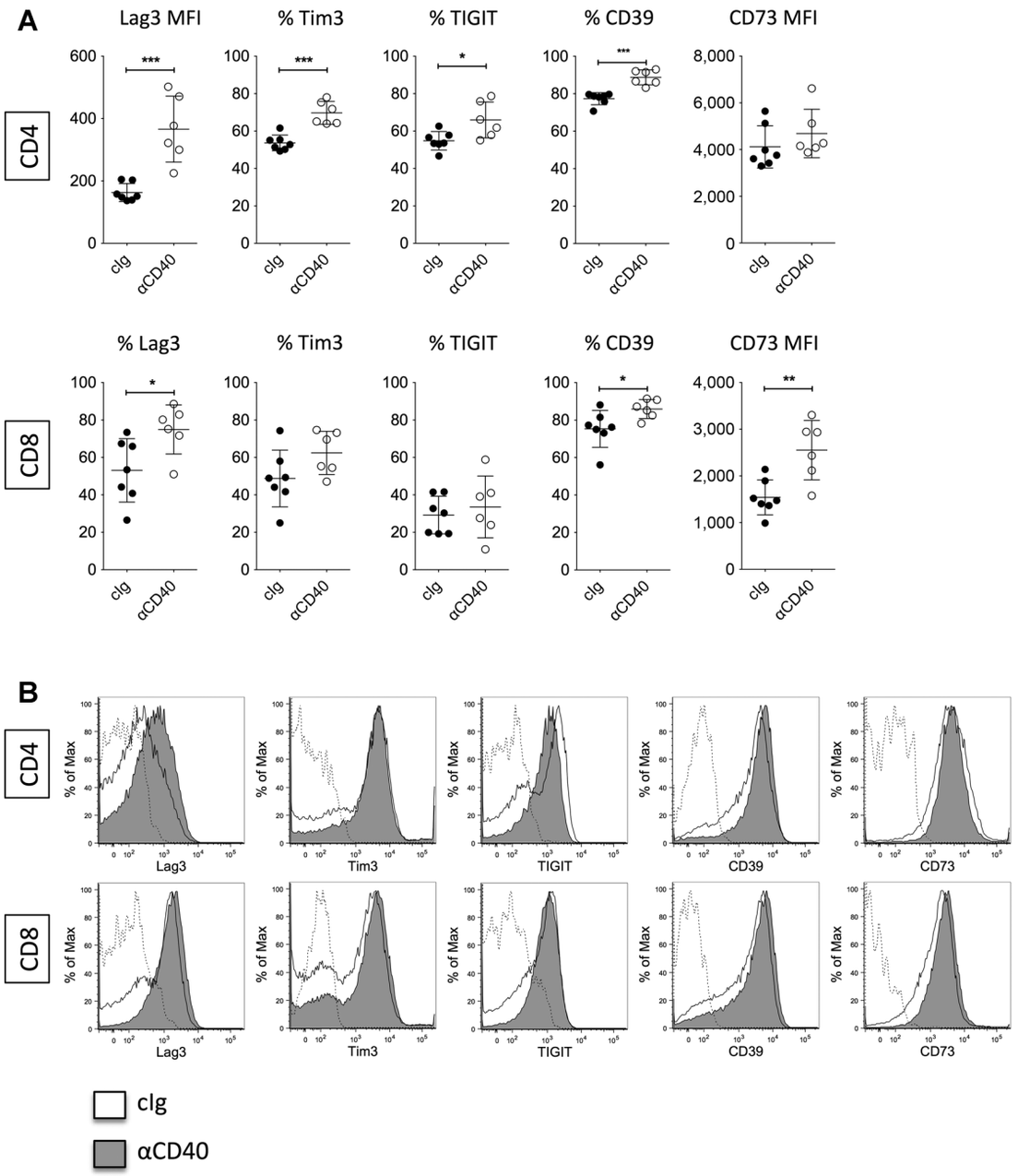

Figure 3.

Anti-CD40 regulates multiple intratumor T-cell checkpoint expression. Groups of B6 WT mice ($n = 6$–7) with established AT3 tumor were treated with cIg or anti-CD40 mAb, and tumors were harvested 2 or 3 days after antibody treatments for flow cytometric analyses. **A,** MFIs of Lag3 and CD73 and frequencies of Lag3$^+$, Tim3$^+$, TIGIT$^+$, and CD39$^+$ in CD4$^+$ (top) and CD8$^+$ (bottom) TILs between cIg- and anti-CD40–treated mice are shown. Data are presented as mean ± SD. Statistical differences in frequencies or MFI between cIg- and anti-CD40–treated mice were determined by an unpaired *t* test (*, $P < 0.05$; **, $P < 0.01$; ***, $P < 0.001$). **B,** concatenated overlaid histogram plots of Lag3, Tim3, TIGIT, CD39, and CD73 of CD4$^+$ (top) and CD8$^+$ (bottom) T cells (dashed histogram, isotype; open histogram, cIg-treated; shaded histogram, anti-CD40–treated) from antibody-treated mice are shown.

Anti-CD40–induced IL12 regulates CD8$^+$ T-cell PD1 expression

Ligation of CD40 on APC is able to induce the production of inflammatory cytokines including IL12 and IL23, serving as a third signal in the generation of a T-cell response (27, 30, 31). Flow cytometry analyses demonstrated that CD11b$^+$ myeloid cell IL12p40 levels were increased in anti-CD40–treated mice (Fig. 5A), indicating an induction of IL12 (IL12p35 and IL12p40 heterodimer) and/or IL23 (IL23p19 and IL12p40 heterodimer) cytokine production (31). To assess whether IL12/23 is involved in regulating T-cell PD1 expression, anti-CD40–treated mice were

Published OnlineFirst September 9, 2016; DOI: 10.1158/0008-5472.CAN-16-2141

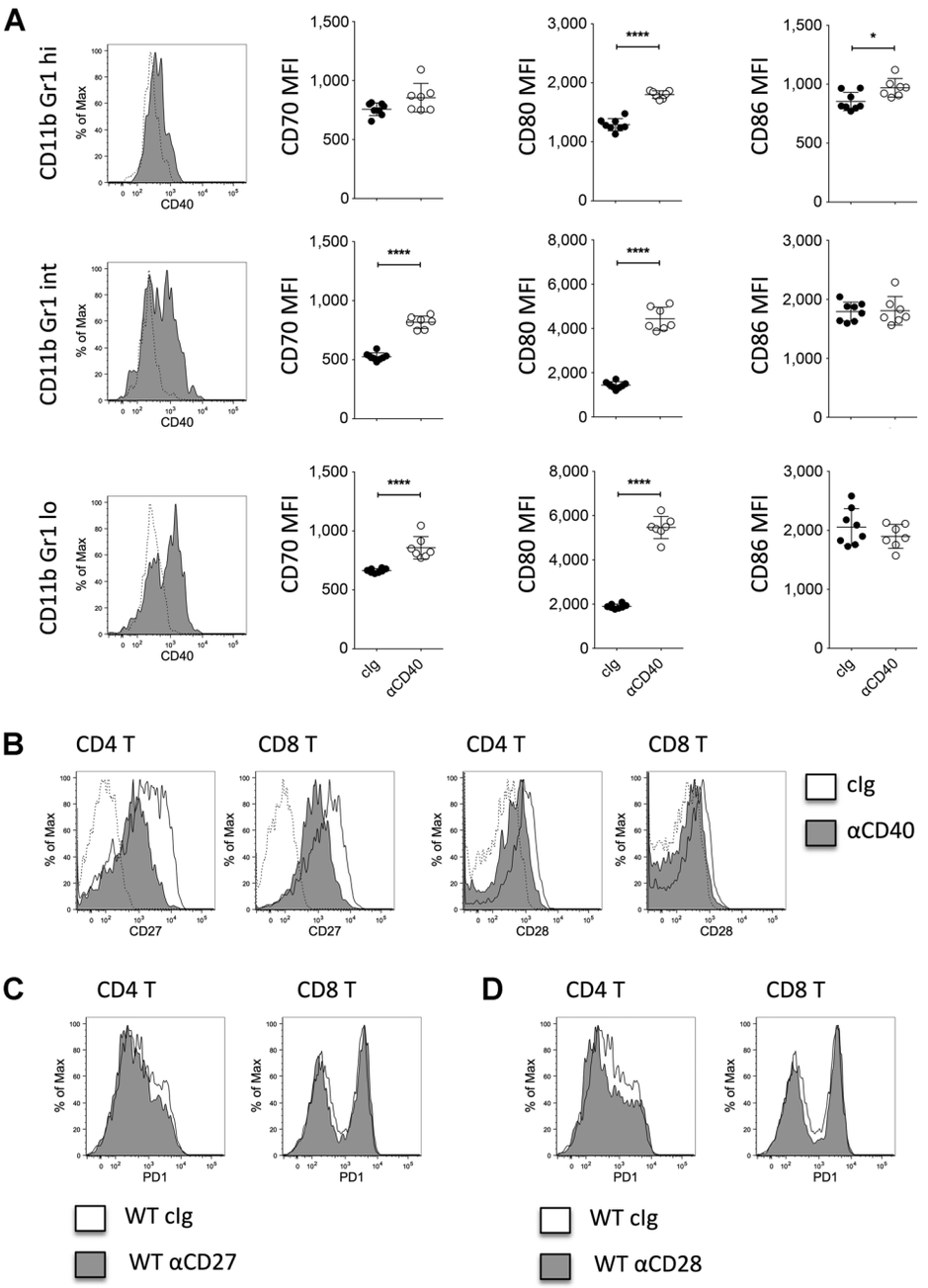

Figure 4.
CD27/CD70 and CD28/CD80/CD86 signaling do not regulate intratumor T-cell PD1 expression. Groups of B6 WT mice ($n = 3$–5) with established AT3 tumor were treated with cIg or anti-CD40 mAb, and tumors were harvested 2 or 3 days after antibody treatments for flow cytometric analyses. **A,** left, representative CD40 histogram plots of CD11b Gr1 subsets of cIg-treated (dashed histogram, isotype; shaded histogram, cIg-treated) mice are shown. Right, CD70, CD80, and CD86 MFIs of CD11b Gr1 subsets between cIg- and anti-CD40–treated mice pooled from two independent experiments are shown. Statistical differences in CD70, CD80, and CD86 MFI of indicated CD11b Gr1 TIL subsets between cIg- and anti-CD40–treated mice were determined by an unpaired t test (*, $P < 0.05$; ****, $P < 0.0001$). **B,** representative overlaid CD27 and CD28 histogram plots of $CD4^+$ and $CD8^+$ T cells (dashed histogram, isotype; open histogram, cIg-treated; shaded histogram, anti-CD40–treated) from antibody-treated mice are shown. **C** and **D,** groups of B6 WT mice ($n = 3$–5) with established AT3 tumor were treated with cIg, anti-CD27, or anti-CD28 mAb, and tumors were harvested 2 or 3 days after antibody treatments for flow cytometric analyses. Representative overlaid PD1 histogram plots of $CD4^+$ and $CD8^+$ T cells (dashed histogram, isotype; open histogram, cIg-treated; shaded histogram, anti-CD27- or anti-CD28–treated) from antibody-treated mice are shown.

coadministered with an anti-IL12p40 neutralizing mAb. Here, we observed a marked rebound of $CD8^+$ T-cell PD1 expression in anti-CD40 + anti-IL12p40–treated mice, abrogating the PD1 downregulation initiated with anti-CD40 mAb alone (Fig. 5B and Supplementary Fig. S5A). To dissect whether anti-CD40–driven IL23 is involved in the downregulation of T-cell PD1 expression, we compared intratumor T cells between cIg- and anti-CD40–treated IL23p19–deficient mice. We found that the anti-CD40–driven $CD8^+$ T-cell PD1 downregulation effect was retained in mice deficient for IL23 (Fig. 5C), implying that IL12 was critical in lowering T-cell PD1 expression. Reciprocally, we treated AT3-bearing mice with recombinant IL12 and observed reduced PD1 expression on $CD8^+$ T cells (Fig. 5D). Interestingly, however, recombinant IL12 therapy had minimal effect in lowering $CD4^+$ T-cell PD1 expression, compared with its effect on $CD8^+$ T cells (Fig. 5D; Supplementary Fig. S5B). This finding concurred with our assessment of PD1 on $CD4^+$ T cells as shown in Fig. 5B, where neutralization of IL12p40 did not result in PD1 recovery (Fig. 5B; Supplementary Fig. S5A). In contrast to IL12, the administration of recombinant IL18 did not downregulate the expression of PD1 on intratumor T cells (Fig. 5E), despite its regulatory role on IL12 receptor expression (32). Thus far, our data showed that anti-CD40–driven IL12 has a primary role in regulating intratumor $CD8^+$ T-cell PD1 expression.

Published OnlineFirst September 9, 2016; DOI: 10.1158/0008-5472.CAN-16-2141

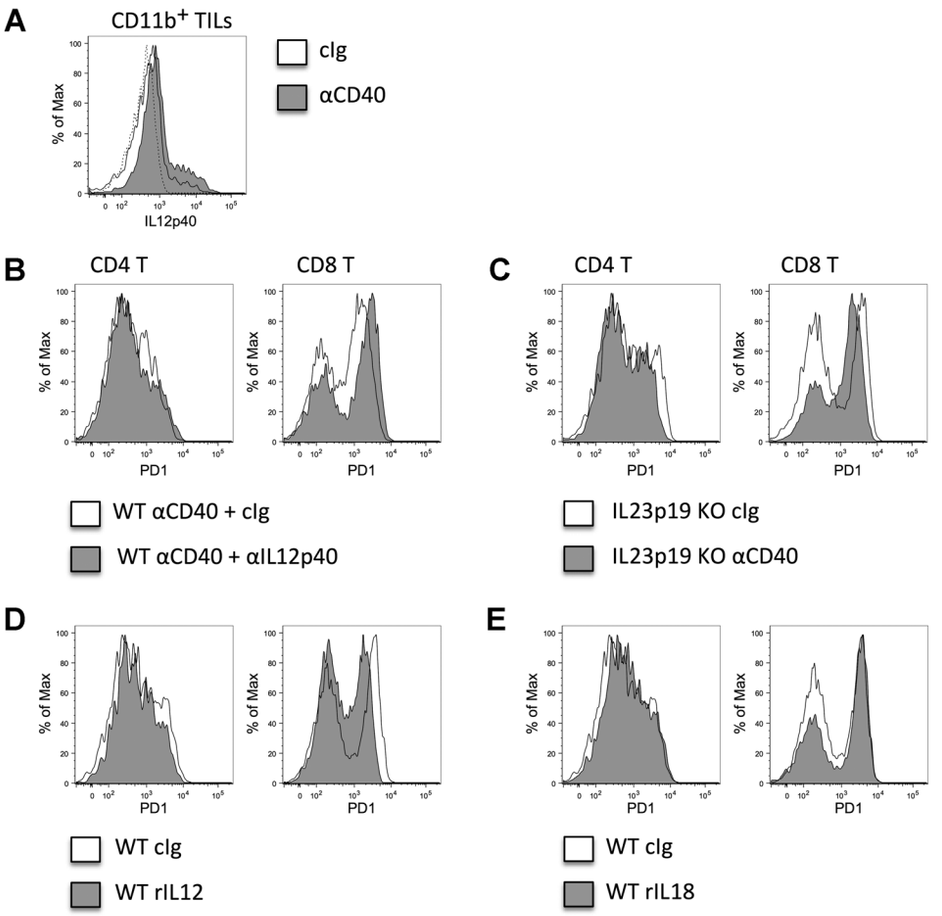

Figure 5.
Anti-CD40–induced IL12 regulates intratumor T-cell PD1 expression. Groups of B6 WT and IL23p19 KO mice ($n = 3$–5) with established AT3 tumor were treated with cIg or anti-CD40 mAb, and tumors were harvested 2 or 3 days after antibody treatments for flow cytometric analyses. **A,** representative IL12p40 overlaid histogram plots of intratumor CD11b$^+$ TILs (dashed histogram, isotype; open histogram, cIg-treated; shaded histogram, anti-CD40–treated) from antibody-treated mice are shown. **B–E,** representative overlaid PD1 histogram plots from antibody- or cytokine-treated mice, as indicated in the figure are shown. Histogram plots of cIg-treated mice are identical between **D** and **E** and Fig. 4C and D.

Anti-CD40 mAb attenuates Treg-suppressive phenotype

We showed that Treg depletion using genetic mouse models (15) or anti-CTLA4 therapy (Supplementary Fig. S1D) could lower CD8$^+$ T-cell PD1 expression. In addition, the increased expression of CD25, CD127, and ICOS on CD4$^+$ T cells also suggested a potential modulation of Treg and/or CTLA4 in responding to the anti-CD40 therapy (33–36). Upon anti-CD40 therapy, we observed a mild increase in the proportion of CD8$^+$ T cells and Tregs (CD4$^+$ Foxp3$^+$), but these changes did not affect the CD8/Treg ratio (Fig. 6A). This observation eliminated the possibility of anti-CD40 mAb directly reducing intratumor Treg to regulate CD8$^+$ T-cell PD1 status. We next asked whether intratumor Tregs were rendered less suppressive following anti-CD40 therapy. Interestingly, we observed that intratumor Treg isolated from anti-CD40–treated mice expressed lower levels of CTLA4 and PD1 (Fig. 6B), indicative of Tregs with attenuated suppressor functions (18, 37–40). In contrast, the proportion of CTLA4-expressing CD4$^+$ Foxp3$^-$ T cells was increased in anti-CD40–treated mice (Fig. 6B). No significant changes were observed for CTLA4-expressing CD8$^+$ T cells between cIg- and anti-CD40–treated mice (Fig. 6B). Our data suggested that anti-CD40 mAb initiated a less suppressive tumor microenvironment for anti-PD1 therapy.

Discussion

It has been recently shown that a combination of ipilimumab and nivolumab, in comparison with nivolumab as a monotherapy, correlated with a better progression-free survival profile in patients with melanoma stained-negative for PDL1 (41). While immunohistochemistry of intratumor T-cell PD1 is not able to distinguish between PD1^{hi} and PD1^{lo} T cells, we reasoned that the high positivity of PDL1 immunohistochemistry staining might be reflective of a PDL1^{hi} and T-cell PD1^{lo} tumor microenvironment. Our current study of the PD1/PDL1 modulatory effect of anti-CTLA4 and anti-CD40 not only confirmed the inverse correlation of T-cell PD1 status to PDL1 expression (PD1^{hi} and PDL1^{lo}; and PD1^{lo} and PDL1^{hi}) in the tumor microenvironment (15), but also suggested a conditioning effect of ipilimumab may be redundant in PDL1-positive tumors. Although one might reason that this PD1/PDL1-modulating effect was driven by the Treg-depleting activity of the anti-mouse CTLA4 mAb, this mechanism is yet to be proven in the patients. However, ipilimumab has been shown capable to trigger an antibody-dependent cell-mediated cytotoxicity (ADCC) effect to kill Treg in an *ex vivo* coculture assay (42). In anti-CD40–treated AT3-bearing mice, we also observed a reduction of CTLA4-expressing intratumor Tregs, likely mimicking the effect of CTLA4 blockade. In this light, the immune modulating effect of ipilimumab as a CTLA4-blocking and/or CTLA4$^+$ Treg-depleting agent is likely beneficial in enhancing anti-PD1 mAb efficacy.

It is important to note that the identification of targets that lower tumor-infiltrating T-cell PD1 expression and enable a synergistic effect with PD1 blockade is likely tumor

Published OnlineFirst September 9, 2016; DOI: 10.1158/0008-5472.CAN-16-2141

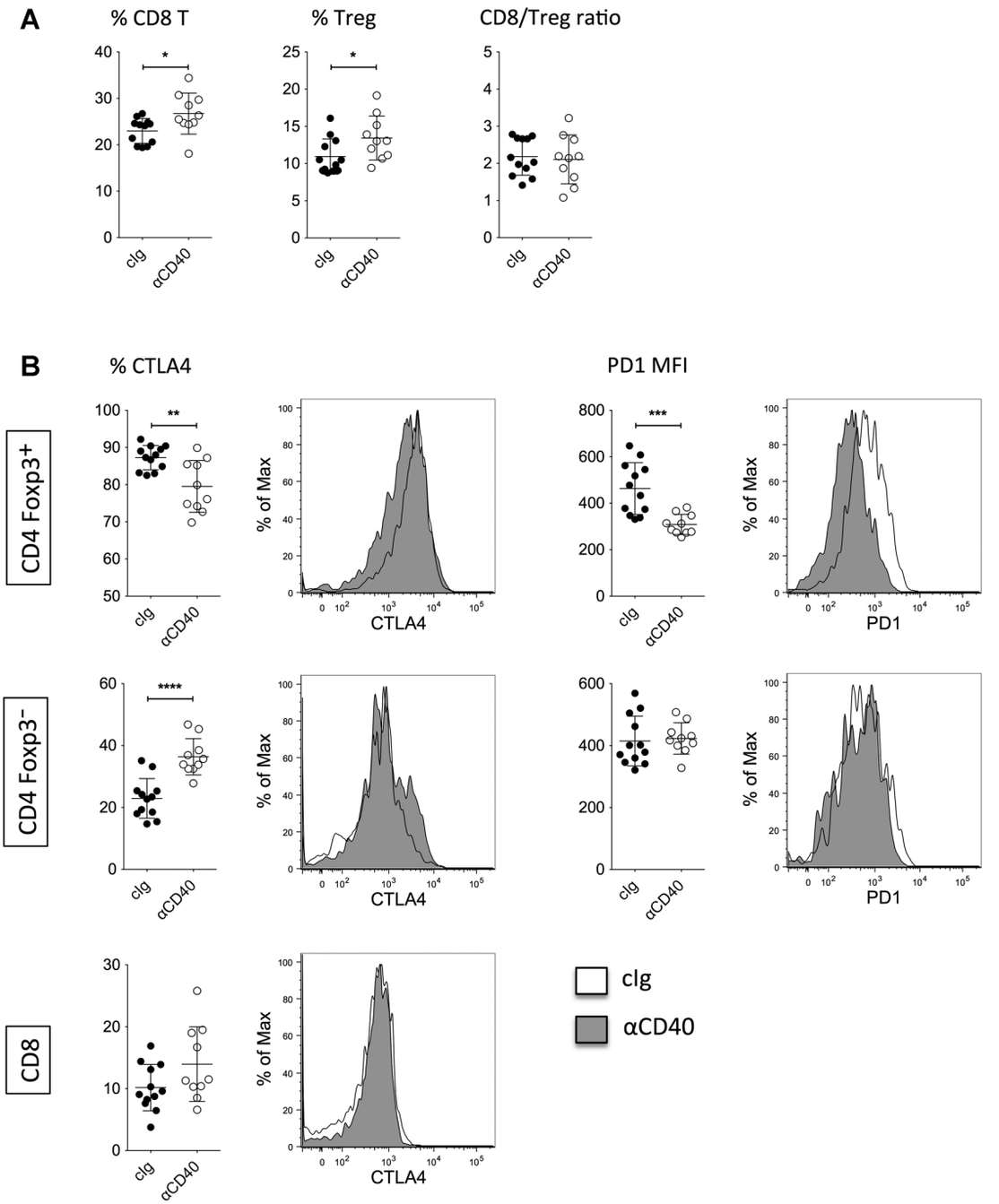

Figure 6.

Anti-CD40 induces intratumor Tregs with an attenuated suppressive phenotype. Groups of B6 WT mice ($n = 3$–5) with established AT3 tumor were treated with clg or anti-CD40 mAb, and tumors were harvested 2 or 3 days after antibody treatments for flow cytometric analyses. **A,** frequencies of $CD8^+$ T cells, Tregs ($CD4^+$ $Foxp3^+$), and CD8/Treg ratio between clg- and anti-CD40–treated mice pooled from three independent experiments are shown. **B,** frequencies of $CTLA4^+$ and MFIs of PD1 for Treg, $CD4^+Foxp3^-$, and $CD8^+$ T cells between clg- and anti-CD40–treated mice pooled from three independent experiments are shown. Representative overlaid CTLA4 and PD1 histogram plots of indicated immune subsets (open histogram, clg-treated; shaded histogram, anti-CD40–treated) from antibody-treated mice are shown. Statistical differences in frequencies, MFI, or CD8/Treg ratio between clg- and anti-CD40–treated mice were determined by an unpaired *t* test (*, $P < 0.05$; **, $P < 0.01$; ***, $P < 0.001$; ****, $P < 0.0001$).

microenvironment-dependent, demonstrated by the contrasting effect of anti-CD40 and anti-PD1 mAbs in AT3- and Renca-bearing mice. While anti-CD40 mAb reduced tumor-infiltrating $CD8^+$ T-cell frequency in Renca tumors, the proportion of $CD8^+$ T cells in AT3 tumors was increased post therapy. We also found that one dose of anti-CD40 mAb was sufficient to

Published OnlineFirst September 9, 2016; DOI: 10.1158/0008-5472.CAN-16-2141

prime a profound antitumor effect in Renca-bearing mice, but not in AT3-bearing mice. It is however not surprising that differing tumor models display diverse responses to combination therapeutic approaches. Despite the clinical success of ipilimumab and nivolumab combination in treating melanoma patients, a proportion of patients remain non-responsive to this combination therapy. In light of our findings, it is of extreme interest to identify factors, other than proportion of T cells and their PD1 status, that dictate the synergistic activity of anti-CD40 and anti-PD1 mAbs in controlling tumor growth.

T-cell exhaustion was first identified in a mouse model of chronic LCMV infection, but this biology was later shown to exist in virus-infected and cancer patients (23, 24). Exhausted $CD8^+$ T cells expressed multiple inhibitory receptors, including PD1 and CTLA4, which regulates the proliferative, cytotoxic, and cytokine-producing capacities of these T cells to eliminate virus-infected or tumor cells. While blockade of PD1/PDL1 could partly reinvigorate T-cell effector functions, only $CD8^+$ T cells marked by $PD1^{lo}$ together with a transcriptional profile of $Tbet^{hi}$ $Eomes^{lo}$ could respond to this therapy (17, 25). The transition of $PD1^{hi}$ to $PD1^{lo}$ expression on $CD8^+$ T cells in anti-CD40–treated mice, together with their transcriptional and functional changes, permitted a reversion of the exhausted T cells and the subsequent antitumor immunity reinvigorated by anti-PD1 mAb. Interestingly, a similar reversion of exhausted $PD1^{hi}$ $CD8^+$ T cells was reported in a mouse model of chronic LCMV infection treated with IL2 therapy (43). Concurring with this finding, our data also showed potential increases of IL2 and IL7, as reflected by the increased CD25 and CD127 expression on intratumor T cells post anti-CD40 therapy. Notably, however, in contrast to West and colleagues (43), we found that anti-CD40 mAb selectively induced Lag3, CD39, and CD73, but not Tim3 or TIGIT expression on $CD8^+$ T cells. Together with the increased PDL1 expression, these changes in inhibitory receptor expression are likely a therapy-induced adaptive resistance mechanism (44). A study of inhibitory pathway dependency as a guide for selecting the most efficacious therapeutic targets to further improve T-cell effector functions is currently under way.

We showed that IL12 has an immediate and primary role in mediating the PD1 modulatory effect of anti-CD40, consistent with its role in regulating Tbet and Eomes expression in $CD8^+$ T cells (23, 45). However, it remains unclear mechanistically why there is a comparatively lower dependency of IL12 in regulating $CD4^+$ T-cell PD1 expression. Nonetheless, this role of IL12 in regulating PD1 expression in exhausted $CD8^+$ T cells appears conserved in different contexts (45–47), highlighting its broad applicability to complement PD1/PDL1 blockade. In this light, a combination of agents that induce IL12 production, including TLR ligands, vaccines, or cellular therapy, are likely to provide benefit with anti-PD1 therapy. Alternatively, restoration of IL12 signaling when anti-PD1 therapy resistance develops may be feasible. Our data also suggest an analysis of CD40/IL12/Tbet-associated signatures in patient sera and/or tissues prior to anti-PD1 therapy may be useful to predict response.

Despite the induction of costimulatory ligands on intratumor myeloid cells after anti-CD40 therapy, we found that activated CD70/CD27 or CD80/CD86/CD28 signaling did not directly downregulate T-cell PD1 expression. Although anti-CD27 agonistic mAb has been reported to reduce intratumor PD1-expressing $CD8^+$ T cells and $Foxp3^+$ Treg in B16-OVA tumors, we did not observe such changes, likely due to the difference in time of analysis (early response versus late response; ref. 48). It is worth noting our data did not exclude the importance of anti-CD40 mAb-driven costimulatory signals in supporting the expansion of effector T cells when anti-PD1 is administered. Similarly, our study did not exclude the potential activity of anti-CD40 mAb in tumor stroma conditioning and activation of tumoricidal macrophages, in driving this PD1 modulatory effect (49). While we did not observe depletion of intratumor Tregs in anti-CD40–treated mice, these Tregs displayed a less activated and less suppressive phenotype. We speculate that these changes in Tregs could be driven by the induction of Tbet, and may result from the interaction between Tregs and APC. However, this cross-talk between APC/Treg/effector T cells remains to be discerned and warrants further assessment.

The development of T-cell checkpoint inhibitors, including anti-PD1 mAbs, to treat cancer is particularly exciting given its efficacy in melanoma patients (2–4, 11, 12, 14). However, a better understanding of PD1 biology is needed to prolong anti-PD1 mAb efficacy and broaden it to other malignancies (12, 50). Using tumor-harboring $PD1^{hi}$ T cells as biomarkers of anti-PD1 therapeutic resistance, we have systematically identified multiple immune conditioning agents that rendered anti-PD1–insensitive T cells to a sensitive phenotype. Of note, our framework of assessing the conversion of $PD1^{hi}$ to $PD1^{lo}$ is not limited to immune-based therapeutic agents, but can be expanded to screening of chemotherapeutic agents, radiotherapy, epigenetic modulators, and small-molecule inhibitors that might potentiate anti-PD1 antitumor response in a previously refractory tumor. In light of the immune conditioning effect of anti-CD40 mAb, the clinical trial results of a combination of anti-CD40 with PD1 or CTLA4 blockade will be of extreme interest (e.g., NCT02706353 and NCT01103635).

Disclosure of Potential Conflicts of Interest

M.W.L. Teng has received speakers bureau honoraria from Merck Sharp & Dohme. A.J. Korman has ownership interest (including patents) in Bristol-Myers Squibb. M.J. Smyth reports receiving a commercial research grant from Bristol-Myers Squibb. No potential conflicts of interest were disclosed by the other authors.

Authors' Contributions

Conception and design: S.F. Ngiow, M.J. Smyth
Development of methodology: S.F. Ngiow, A. Young
Acquisition of data (provided animals, acquired and managed patients, provided facilities, etc.): S.F. Ngiow, A. Young, S.J. Blake, M.J. Smyth
Analysis and interpretation of data (e.g., statistical analysis, biostatistics, computational analysis): S.F. Ngiow, A. Young M.J. Smyth
Writing, review, and/or revision of the manuscript: S.F. Ngiow, A. Young, S.J. Blake, G.R. Hill, H. Yagita, M.W.L. Teng, A.J. Korman, M.J. Smyth
Administrative, technical, or material support (i.e., reporting or organizing data, constructing databases): S.F. Ngiow, H. Yagita
Study supervision: S.F. Ngiow, M.W.L. Teng, M.J. Smyth
Other (provided antibody and experimental design): A.J. Korman

Acknowledgments

The authors wish to thank Liam Town, Kate Elder, and Joanne Sutton for breeding, genotyping, and maintenance and care of the mice used in this study.

Grant Support

S.F. Ngiow, A. Young, and M.J. Smyth were supported by a National Health and Medical Research Council of Australia (NH&MRC) Australia Fellowship (628623) and Senior Principal Research Fellowship (1078671), and a QIMR Berghofer Ride to Conquer Cancer Grant. G.R. Hill is a NH&MRC Senior

Published OnlineFirst September 9, 2016; DOI: 10.1158/0008-5472.CAN-16-2141

Principal Research Fellow. S.F. Ngiow was supported by a NH&MRC CJ Martin Fellowship (1111469). A. Young was supported by a Cancer Council Queensland Ph.D. Fellowship. S.J. Blake and M.W.L. Teng were supported by an NH&MRC CDF1 (1025552) and project grant (1059862). H. Yagita was supported by a grant (26290059) from MEXT, Japan.

The costs of publication of this article were defrayed in part by the payment of page charges. This article must therefore be hereby marked *advertisement* in accordance with 18 U.S.C. Section 1734 solely to indicate this fact.

Received August 4, 2016; accepted August 26, 2016; published OnlineFirst September 9, 2016.

References

1. Ansell SM, Lesokhin AM, Borrello I, Halwani A, Scott EC, Gutierrez M, et al. PD-1 blockade with nivolumab in relapsed or refractory Hodgkin's lymphoma. N Engl J Med 2015;372:311–9.
2. Hamid O, Robert C, Daud A, Hodi FS, Hwu W-J, Kefford R, et al. Safety and tumor responses with lambrolizumab (anti-PD-1) in melanoma. N Engl J Med 2013;369:134–44.
3. Robert C, Long GV, Brady B, Dutriaux C, Maio M, Mortier L, et al. Nivolumab in previously untreated melanoma without BRAF mutation. N Engl J Med 2015;372:320–30.
4. Topalian SL, Hodi FS, Brahmer JR, Gettinger SN, Smith DC, McDermott DF, et al. Safety, activity, and immune correlates of anti-PD-1 antibody in cancer. N Engl J Med 2012;366:2443–54.
5. Tumeh PC, Harview CL, Yearley JH, Shintaku IP, Taylor EJM, Robert L, et al. PD-1 blockade induces responses by inhibiting adaptive immune resistance. Nature 2014;515:568–71.
6. Nghiem PT, Bhatia S, Lipson EJ, Kudchadkar RR, Miller NJ, Annamalai L, et al. PD-1 blockade with pembrolizumab in advanced Merkel-cell carcinoma. N Engl J Med 2016;374:2542–52.
7. Rizvi NA, Hellmann MD, Snyder A, Kvistborg P, Makarov V, Havel JJ, et al. Mutational landscape determines sensitivity to PD-1 blockade in non–small cell lung cancer. Science 2015;348:124–8.
8. Le DT, Uram JN, Wang H, Bartlett BR, Kemberling H, Eyring AD, et al. PD-1 blockade in tumors with mismatch-repair deficiency. N Engl J Med 2015;372:2509–20.
9. McGranahan N, Furness AJ, Rosenthal R, Ramskov S, Lyngaa R, Saini SK, et al. Clonal neoantigens elicit T cell immunoreactivity and sensitivity to immune checkpoint blockade. Science 2016;351:1463–9.
10. Gubin MM, Zhang X, Schuster H, Caron E, Ward JP, Noguchi T, et al. Checkpoint blockade cancer immunotherapy targets tumour-specific mutant antigens. Nature 2014;515:577–81.
11. Pardoll DM. The blockade of immune checkpoints in cancer immunotherapy. Nat Rev Cancer 2012;12:252–64.
12. Smyth MJ, Ngiow SF, Ribas A, Teng MWL. Combination cancer immunotherapies tailored to the tumour microenvironment. Nat Rev Clin Oncol 2016;13:143–58.
13. Sharma P, Allison JP. Immune checkpoint targeting in cancer therapy: toward combination strategies with curative potential. Cell 2015;161:205–14.
14. Khalil DN, Smith EL, Brentjens RJ, Wolchok JD. The future of cancer treatment: immunomodulation, CARs and combination immunotherapy. Nat Rev Clin Oncol 2016;13:394.
15. Ngiow SF, Young A, Jacquelot N, Yamazaki T, Enot D, Zitvogel L, et al. A threshold level of intratumor CD8+ T-cell PD1 expression dictates therapeutic response to anti-PD1. Cancer Res 2015;75:3800–11.
16. Thommen DS, Schreiner J, Müller P, Herzig P, Roller A, Belousov A, et al. Progression of lung cancer is associated with increased dysfunction of T Cells defined by coexpression of multiple inhibitory receptors. Cancer Immunol Res 2015;3:1344–55.
17. Blackburn SD, Shin H, Freeman GJ, Wherry EJ. Selective expansion of a subset of exhausted CD8 T cells by αPD-L1 blockade. Proc Natl Acad Sci U S A 2008;105:15016–21.
18. Penaloza-MacMaster P, Kamphorst AO, Wieland A, Araki K, Iyer SS, West EE, et al. Interplay between regulatory T cells and PD-1 in modulating T cell exhaustion and viral control during chronic LCMV infection. J Exp Med 2014;211:1905–18.
19. Teng MWL, Andrews DM, McLaughlin N, von Scheidt B, Ngiow SF, Möller A, et al. IL-23 suppresses innate immune response independently of IL-17A during carcinogenesis and metastasis. Proc Natl Acad Sci 2010;107:8328–33.
20. Ngiow SF, von Scheidt B, Akiba H, Yagita H, Teng MWL, Smyth MJ. Anti-TIM3 antibody promotes T cell IFN-γ-mediated antitumor immunity and suppresses established tumors. Cancer Res 2011;71:3540–51.
21. Sakuishi K, Ngiow SF, Sullivan JM, Teng MWL, Kuchroo VK, Smyth MJ, et al. TIM3+FOXP3+ regulatory T cells are tissue-specific promoters of T-cell dysfunction in cancer. OncoImmunology 2013;2:e23849.
22. Selby MJ, Engelhardt JJ, Quigley M, Henning KA, Chen T, Srinivasan M, et al. Anti-CTLA-4 antibodies of IgG2a isotype enhance antitumor activity through reduction of intratumoral regulatory T cells. Cancer Immunol Res 2013;1:32–42.
23. Wherry EJ, Kurachi M. Molecular and cellular insights into T cell exhaustion. Nat Rev Immunol 2015;15:486–99.
24. Pauken KE, Wherry EJ. Overcoming T cell exhaustion in infection and cancer. Trends Immunol 2015;36:265–76.
25. Paley MA, Kroy DC, Odorizzi PM, Johnnidis JB, Dolfi DV, Barnett BE, et al. Progenitor and terminal subsets of CD8+ T cells cooperate to contain chronic viral infection. Science 2012;338:1220–5.
26. Blackburn SD, Shin H, Haining WN, Zou T, Workman CJ, Polley A, et al. Coregulation of CD8+ T cell exhaustion by multiple inhibitory receptors during chronic viral infection. Nat Immunol 2009;10:29–37.
27. Elgueta R, Benson MJ, de Vries VC, Wasiuk A, Guo Y, Noelle RJ. Molecular mechanism and function of CD40/CD40L engagement in the immune system. Immunol Rev 2009;229:152–72.
28. Bullock TNJ, Yagita H. Induction of CD70 on dendritic cells through CD40 or TLR stimulation contributes to the development of CD8+ T cell responses in the absence of CD4+ T cells. J Immunol 2005;174:710–7.
29. Cella M, Scheidegger D, Palmer-Lehmann K, Lane P, Lanzavecchia A, Alber G. Ligation of CD40 on dendritic cells triggers production of high levels of interleukin-12 and enhances T cell stimulatory capacity: T-T help via APC activation. J Exp Med 1996;184:747–52.
30. Curtsinger JM, Mescher MF. Inflammatory cytokines as a third signal for T cell activation. Curr Opin Immunol 2010;22:333–40.
31. Ngiow SF, Teng MWL, Smyth MJ. A balance of interleukin-12 and -23 in cancer. Trends Immunol 2013;34:548–55.
32. Fantuzzi L, Puddu P, Varano B, Del Cornò M, Belardelli F, Gessani S. IFN-α and IL-18 exert opposite regulatory effects on the IL-12 receptor expression and IL-12-induced IFN-γ production in mouse macrophages: novel pathways in the regulation of the inflammatory response of macrophages. J Leukoc Biol 2000;68:707–14.
33. Hannani D, Vetizou M, Enot D, Rusakiewicz S, Chaput N, Klatzmann D, et al. Anticancer immunotherapy by CTLA-4 blockade: obligatory contribution of IL-2 receptors and negative prognostic impact of soluble CD25. Cell Res 2015;25:208–24.
34. Mazzucchelli R, Hixon JA, Spolski R, Chen X, Li WQ, Hall VL, et al. Development of regulatory T cells requires IL-7Rα stimulation by IL-7 or TSLP. Blood 2008;112:3283–92.
35. Riley JL, Blair PJ, Musser JT, Abe R, Tezuka K, Tsuji T, et al. ICOS costimulation requires IL-2 and can be prevented by CTLA-4 engagement. J Immunol 2001;166:4943–8.
36. Rudd CE, Schneider H. Unifying concepts in CD28, ICOS and CTLA4 co-receptor signalling. Nat Rev Immunol 2003;3:544–56.
37. Park HJ, Park JS, Jeong YH, Son J, Ban YH, Lee B-H, et al. PD-1 Upregulated on regulatory T cells during chronic virus infection enhances the suppression of CD8+ T cell immune response via the interaction with PD-L1 expressed on CD8+ T cells. J Immunol 2015;194:5801–11.
38. Teng MWL, Ritchie DS, Neeson P, Smyth MJ. Biology and clinical observations of regulatory T cells in cancer immunology. In: Dranoff G, editor. Cancer Immunology and Immunotherapy. Berlin, Heidelberg: Springer Berlin Heidelberg; 2011. p. 61–95.

39. Wang W, Lau R, Yu D, Zhu W, Korman A, Weber J. PD1 blockade reverses the suppression of melanoma antigen-specific CTL by CD4+CD25Hi regulatory T cells. Int Immunol 2009;21:1065–77.
40. Josefowicz SZ, Lu LF, Rudensky AY. Regulatory T cells: mechanisms of differentiation and function. Annu Rev Immunol 2012;30:531–64.
41. Larkin J, Chiarion-Sileni V, Gonzalez R, Grob JJ, Cowey CL, Lao CD, et al. Combined nivolumab and ipilimumab or monotherapy in untreated melanoma. N Engl J Med 2015;373:23–34.
42. Romano E, Kusio-Kobialka M, Foukas PG, Baumgaertner P, Meyer C, Ballabeni P, et al. Ipilimumab-dependent cell-mediated cytotoxicity of regulatory T cells ex vivo by nonclassical monocytes in melanoma patients. Proc Natl Acad Sci U S A 2015;112:6140–5.
43. West EE, Jin HT, Rasheed AU, Penaloza-Macmaster P, Ha SJ, Tan WG, et al. PD-L1 blockade synergizes with IL-2 therapy in reinvigorating exhausted T cells. J Clin Invest 2013;123:2604–15.
44. Zippelius A, Schreiner J, Herzig P, Muller P. Induced PD-L1 expression mediates acquired resistance to agonistic anti-CD40 treatment. Cancer Immunol Res 2015;3:236–44.
45. Takemoto N, Intlekofer AM, Northrup JT, Wherry EJ, Reiner SL. Cutting Edge: IL-12 inversely regulates T-bet and eomesodermin expression during pathogen-induced CD8+ T cell differentiation. J Immunol 2006;177:7515–9.
46. Gerner MY, Heltemes-Harris LM, Fife BT, Mescher MF. Cutting Edge: IL-12 and type I IFN differentially program CD8 T cells for programmed death 1 re-expression levels and tumor control. J Immunol 2013;191:1011–5.
47. Schurich A, Pallett LJ, Lubowiecki M, Singh HD, Gill US, Kennedy PT, et al. The third signal cytokine IL-12 rescues the anti-viral function of exhausted HBV-specific CD8 T cells. PLoS Pathogens 2013;9:e1003208.
48. Roberts DJ, Franklin NA, Kingeter LM, Yagita H, Tutt AL, Glennie MJ, et al. Control of established melanoma by CD27 stimulation is associated with enhanced effector function and persistence, and reduced PD-1 expression of tumor infiltrating CD8+ T cells. J Immunother 2010;33:769–79.
49. Beatty GL, Chiorean EG, Fishman MP, Saboury B, Teitelbaum UR, Sun W, et al. CD40 agonists alter tumor stroma and show efficacy against pancreatic carcinoma in mice and humans. Science 2011;331:1612–6.
50. Teng MW, Ngiow SF, Ribas A, Smyth MJ. Classifying cancers based on T-cell infiltration and PD-L1. Cancer Res 2015;75:2139–45.

Published OnlineFirst September 9, 2016; DOI: 10.1158/0008-5472.CAN-16-2141

Cancer Research
The Journal of Cancer Research (1916–1930) | The American Journal of Cancer (1931–1940)

AACR American Association for Cancer Research

Agonistic CD40 mAb-Driven IL12 Reverses Resistance to Anti-PD1 in a T-cell–Rich Tumor

Shin Foong Ngiow, Arabella Young, Stephen J. Blake, et al.

Cancer Res 2016;76:6266-6277. Published OnlineFirst September 9, 2016.